CHAPTER IV
RESULTS AND DISCUSSION

4.1 Pressure Decay Curves

The pressure decay of CO_2 from 400 psi to 950 psi at 30 °C in crude oil API 62.1, n-pentane and n-heptane are shown in Fig 4.1 – Fig. 4.5.

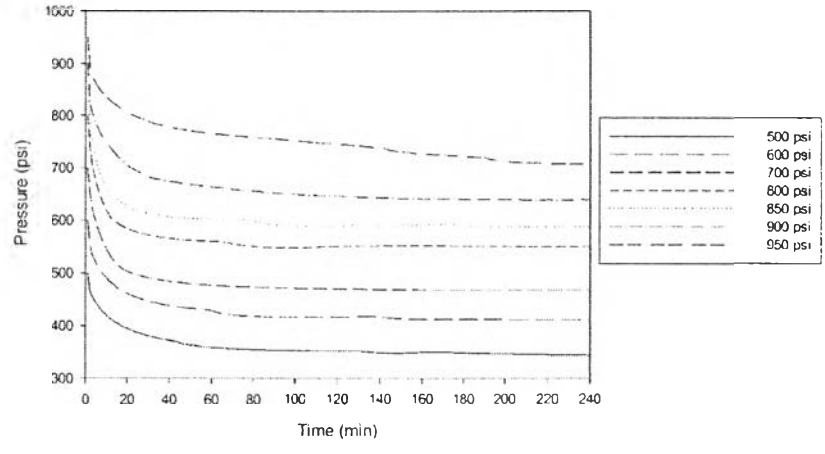

Figure 4.1 Pressure decay curves of crude oil API 62.1 at 30 °C.

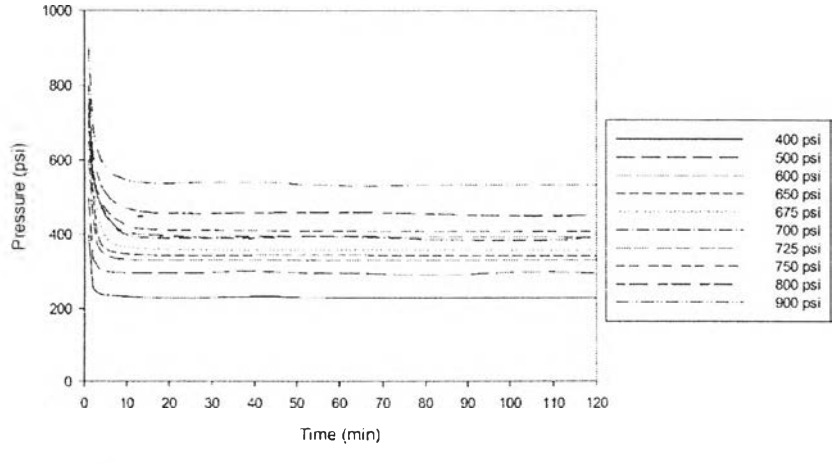

Figure 4.2 Pressure decay curves of n-pentane (C_5) at 30 °C.

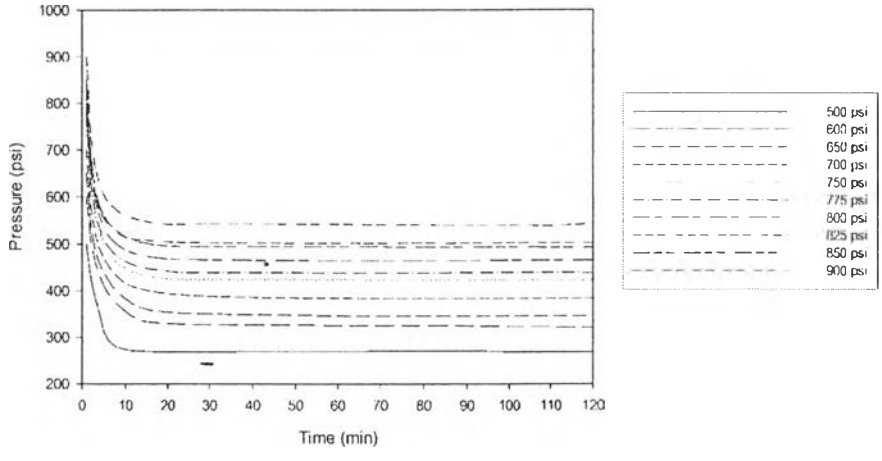

Figure 4.3 Pressure decay curves of n-heptane (C_7) at 30 °C.

The average injection time of CO_2 gas in crude oil API 62.1, n-pentane and n-heptane at 30 °C were 22.66 ± 3.66, 19.40 ± 3.60 and 20.72 ± 2.91 second, respectively. After injecting CO_2 gas into the reactor, CO_2 rapidly diffuses into oil as seen by the pressure inside the reactor rapidly decreases at the initial time and gradually decreases to reach the equilibrium. It indicates that the mass transfer of CO_2 from gas phase into the hydrocarbon phase at the initial state was faster than the later state. The time for CO_2 diffusion to reach the equilibrium of crude oil API 62.1, n-pentane and n-heptane were 40, 10 and 20 min, respectively.

The different equilibrium time for different hydrocarbons indicated different molecular weight of petroleum crude. Crude oil API 62.1 took the longest time, and that of n-heptane was longer than n-pentane Increase of molecular weight (C_5 to C_7) increase the time for the system to reach the equilibrium. In addition, the lower oil viscosity, in this case n-pentane is the lowest, is beneficial to get faster speed of CO_2 diffuse into the oil phase (Song *et al.*, 2010).

The effect of temperature was studied using crude oil API 62.1 and n-heptane. When the pressure decay was determined at 40 °C as the result shown in Fig. 4.4 and Fig. 4.5, respectively. The average injection time of CO_2 gas in crude oil API 62.1 was 22.62 ± 4.18 second, and 21.43 ± 4.00 second for n-heptane. The pressure decay reaches equilibrium around 20 min for crude oil system and 10 min for n-heptane system. When the temperature was increase from 30 °C to 40 °C, CO_2

could diffuse into the oil faster than low temperature at 30 °C. The oil viscosity was decrease with the increase of temperature. CO_2 can diffuse into the low viscosity oil faster than the high viscosity oil. At the higher temperature, the system between CO_2 and hydrocarbon will reach the equilibrium faster.

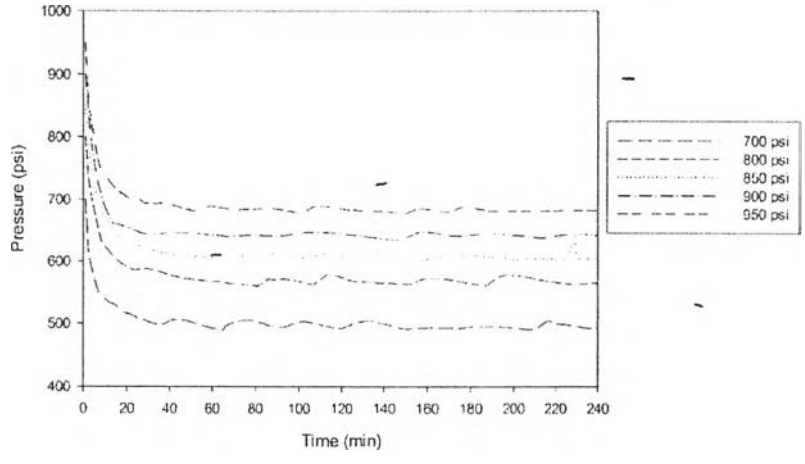

Figure 4.4 Pressure decay curve of crude oil API 62.1 at 40 °C.

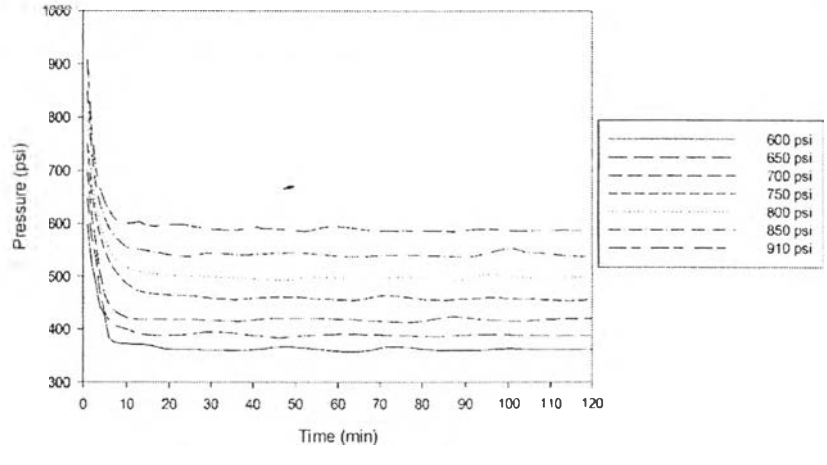

Figure 4.5 Pressure decay curve of n-heptane (C_7) at 40 °C.

4.2 Pressure Drop Curves

The total pressure drop was plotted against the initial pressure as shown in Fig. 4.7 to Fig. 4.9. The results show the total pressure drop increases as the initial pressure is increased and reaches the maximum at 890 psi for crude oil API 62.1, 680 psi for C_5 and 785 psi for C_7 at 30 °C measurement.

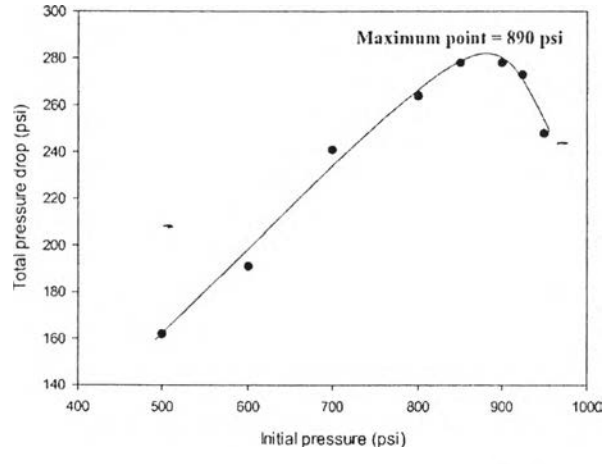

Figure. 4.6 Pressure drop curve of crude oil API 62.1 at 30 °C.

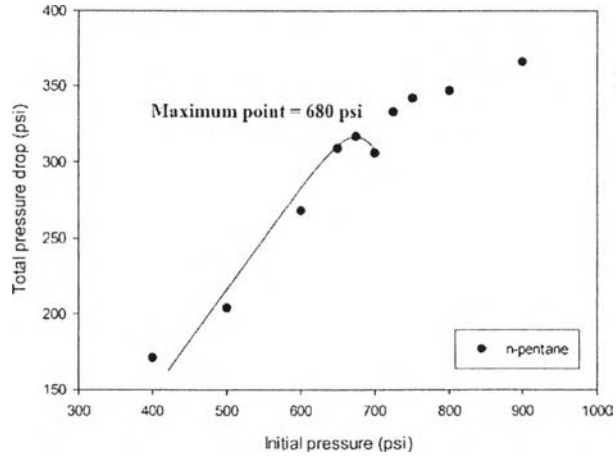

Figure 4.7 Pressure drop curve of n-pentane (C_5) at 30 °C.

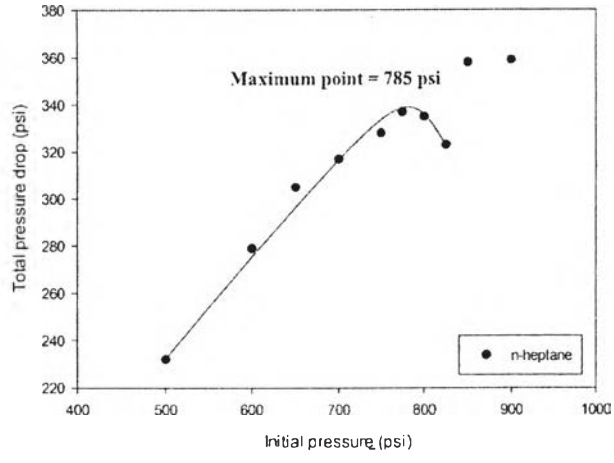

Figure 4.8 Pressure drop curve of n-heptane (C_7) at 30 °C.

In the plot of the total pressure drop against the initial pressure, there are two important regions where the total pressure drop increase, reach maximum, and decrease as the initial pressure increased due to different mechanisms involved. The first region, which the total pressure drop was increase with the initial pressure, is involved the immiscibility between CO_2 and hydrocarbon CO_2 created the boundary layer at the interface between crude oil (liquid phase) and CO_2 (gas phase). The boundary layer limited the movement of CO_2 and the crude oil inside the reservoir and giving a low oil recovery. The maximum point in the pressure drop curve was proposed to be the MMP point of the system, however, it requires the other MMP measured experiment to confirm the result.

4.3 Support the Proposed of MMP

To support the proposed results of MMP in this study, a reference oil was used to measure the MMP value by the pressure decay method and the result was compared with the literature. Yong-Chen et al. (2011) measured the MMP of the CO_2 and n-decane (C_{10}) system at 20 °C using magnetic resonance imaging (MRI) technique and the MMP measured was 818 psi.

In this work, the total pressure drop plotted against the initial pressure of CO_2 for the CO_2- n-decane system at 20 °C shown in Fig. 4.9 and the maximum point at first state of the curve is 820 psi, and comparison of the results is shown in Table 4.1 with the percent absolute deviation (%AD) of 0.24%. Yong-Chen *et al.* (2011) reported the MMP of n-decane of 818 psi which determined the MMP of CO_2 and n-decane system at 20 °C by the magnetic resonance imaging (MRI) technique. Thus, the maximum total pressure drop of n-decane in the pressure drop curve as shown in Fig. 4.11 indicated the MMP of n-decane at 20 °C. For the system of CO_2-crude oil API 62.1, CO_2-n-pentane and CO_2-n-heptane, the MMP point at 30 °C which could be interpreted in the similar manner to the CO_2-n-decane system were 890 psi, 680 psi and 785 psi, respectively.

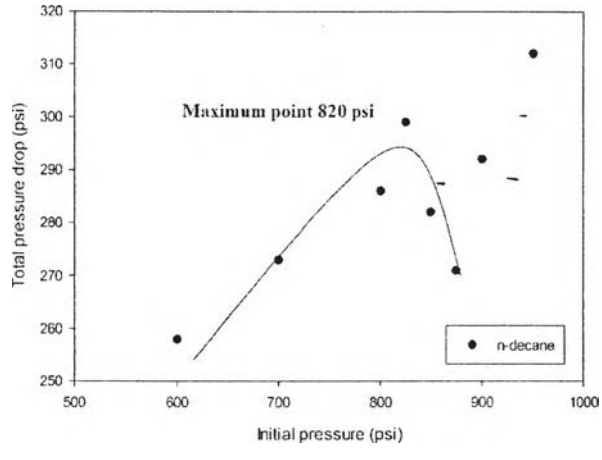

Figure 4.9 Pressure drop curve of n-decane at 20 °C.

Table 4.1 Comparison of MMP from this work with Yong-Chen *et al.* (2011)

Experiment	MMP of n-decane/CO_2 at 20 °C (psi)	%AD (%)
This work	820	-
Yong-Chen *et al.* (2011)	818	0.24

4.3.1 Component of Pressure Drop Curves

In the pressure drop curve could be separate to be three regions. In the first region, as the total pressure drop increases with the initial pressure, it is related to the immiscibility of the gas in the oil phase as illustrated in Fig. 4.10 (a). CO_2 gas is bubbled and dispersed into the oil phase causing the oil to swell as illustrated in Fig. 4.10 (b) which could be compared to oil being stabilized in the surfactant phase of emulsion in the surfactant flooding mechanism. As the results, the volume of oil phase increases and the oil viscosity reduces, this evidence of oil swelling is reported by Abedini and Torabi (2013).The amount of oil swelling could be determined by the swelling factor (SF) and a plot of SF against equilibrium pressure. The plot between the total pressure drop plot could be compared with the plot of SF where the initial stage of total pressure drop curve was increase with the increase of the initial pressure due to the increase of the mass transfer of CO_2 causing the oil to swell. The higher the total pressure drop increases, the more gas dispersing in the oil. Further increase the initial pressure, the total pressure drop reaches the maximum point. Accordingly, the sizes of the bubbles of gas are also decrease as the pressure increases as illustrated in Fig. 4.10 (c) and eventually vanished where the interfacial tension of gas-oil (γ_{go}) is disappear, thus, the immiscibility of CO_2 and the oil is also vanished which takes place at the total pressure drop reaching maximum point and the mechanism of gas beyond this point is involved the diffusion of CO_2 in the oil phase.

The second region of the swelling factor curve is the reduction of swelling factor because the oil volume decreases due to the light component of crude oil vaporized. The increase of CO_2 pressure increases the amount of extracted oil, and the extraction is continued until the system achieved the miscibility. The MMP

point at the SF curve was the intersection between second stage (SF decrease with high slope) and third stage (SF is slightly decrease) of SF curve. It's different to the second region of the pressure drop curve. For the second region of the pressure drop curve was involved the diffusion of CO_2, further increase the initial pressure may cause the light components in the oil to release into the gas phase as illustrated in Fig. 4.10 (d), thus creates gas mixture in the system. Then, the gas mixture was injected and diffused into the oil phase by the first contact miscibility (FCM) or the multiple contact miscibility (MCM). After the system became miscible condition as illustrated in Fig. 4.10 (e), the total pressure drop was decrease. Increase of the initial pressure possibly expanded the miscible phase until the system became a full miscibility as illustrated in Fig. 4.10 (f). At the maximum point of total pressure drop, it was proposed due to a miscible condition between CO_2 and hydrocarbon after the total pressure drop curve was pass the maximum point.

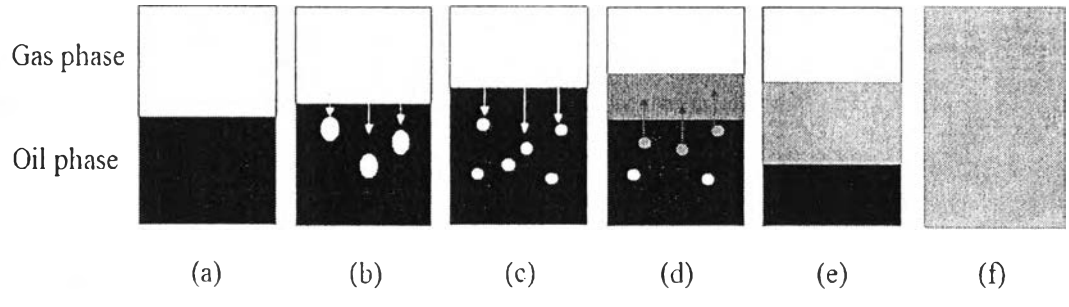

Figure 4.10 Compare the mechanism of miscibility in oil-CO_2 system to the mechanism of emulsion, effect of pressure increase from (a) to (f).

And the third region was the extension of the pressure drop curve, at above the maximum point. Fig. 4.7 and Fig. 4.8 show the results of the total pressure drop increase again for n-pentane and n-heptane systems as the initial pressure was higher than the maximum point around 50 psi. The increase of total pressure drop above the maximum point could occur by the different phase conditions of below and above the miscible conditions making the diffusion phenomena of gas into the liquid change. In the immiscible condition (below the maximum point), CO_2 and liquid

hydrocarbon were in the two phases. CO_2 diffused into the liquid until it reached the equilibrium. After reaching the miscible condition, CO_2 and liquid hydrocarbon form the single one phase. The mechanism of the CO_2 diffusion was changed. And after the system created the miscible phase like Fig. 4.10 (e), it was possible that the increase of initial pressure expanded the miscible phase until the system was fully a single phase as illustrated in Fig. 4.10 (f).

4.3.2 Change in Diffusion Mechanism

To support the change in diffusion mechanism, the pressure decay curve below (at 650 psi) and above (at 700 psi) the maximum point from pressure drop curve of CO_2-n-pentane system is shown in Fig. 4.11. The shape of pressure decay curve below the maximum point of n-pentane at 30 °C look like the normal pressure decay curve (exponential curve). The pressure decay at the first stage takes around 3 min before its change to the next state by changing the slope of the curve. For the plot above the maximum point of n-pentane at 30 °C, the first state of pressure decay took shorter time than (2 min). At below the maximum point it takes time in the first stage higher than above the maximum point due to the slope which the slope of below the maximum point curve was lower. The shape of pressure decay curve and the slope of the curve was result of the different mechanism of CO_2 diffusion into the crude oil phase.

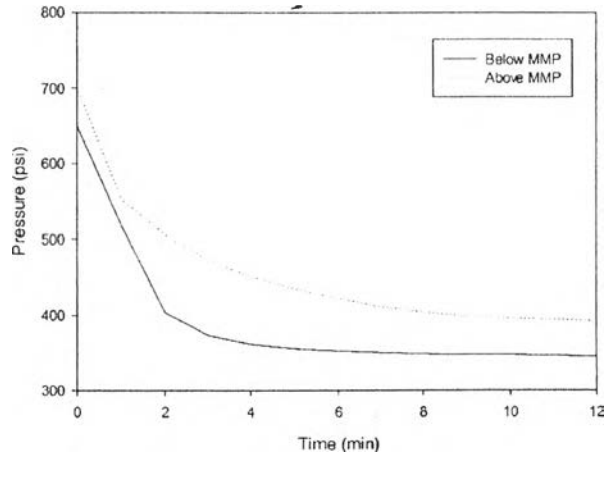

Figure 4.11 Pressure decay curve of n-pentane at 30 °C and below and above the maximum point in pressure drop curve.

4.3.3 Mechanism of MMP

The miscibility mechanism of CO_2 and crude oil system might be similar to the mechanism of surfactant flooding. The surfactant forms micelles with oil and disperses in the water phase similar to the CO_2 bubbles diffusing in the oil phase. The CO_2 diffusion increases the volume of the other phase and decrease in the interfacial tension. Increase of the surfactant concentration increases the driving force and the amount of oil solubilizing in the micelle. Similarly, the increase of CO_2 pressure increases the amount of CO_2 diffusion into the oil until the system form the miscible zone. The miscible zone of CO_2 and crude oil system could be the first contact miscibility (FCM) or multiple contact miscibility (MCM) depending on its pseudo-ternary diagram. However, the FCM generally happens at higher pressure than the MCM condition. Thus, the MCM was most likely happening with the CO_2-crude API 62.1 system and possibly could be described by the pseudo-ternary phase diagram which can be described by mole percentages of three components, mol% of CO_2, mol% of intermediate component (C_2-C_6) and mol% of C_{7+}. The composition of crude API 62.1 shown in Table 4.2 consists of no C_1, 9.19 % mole of C_2-C_6 and 90.81 %mole of C_{7+}. The pseudo-ternary phase diagram in this study was not determined, but could be described in the similar manner to that reported by Jütner (1997) which the mechanism of the system was concluded to be the vaporizing gas drive.

For hydrocarbon systems (CO_2-C_5, CO_2-C_7), the immiscible condition was the same concept as the crude oil system. The miscibility occurred when the hydrocarbon gas completely dissolves into the CO_2 (Yong-Chen *et al.*, 2011). The binary phase diagram can be used to predict the FCM which happen at the condition above the critical point which was varied with temperature (Yu *et al.*, 2006). The system which the pressure is higher than the critical point at its temperature will be the miscible condition and below the critical point, will be the MCM, but the mechanism, condensing gas drive or vaporizing gas drive, could not be identified.

Table 4.2 Oil compositions of crude oil

API gravity	62.1
Specific gravity	0.7301
Average molecular weight	154
MW_{C7+}	145.19
Mol% of C_1	0
Mol% of C_2-C_6	9.19
Mol% of C_{7+}	90.81

4.4 Effect of Molecular Weight.

Effect of molecular weight of oil on MMP was studied using three different liquid hydrocarbon samples as shown in Table 4.3 and Fig. 4.12.

Table. 4.3 Effect of molecular weight on MMP of CO_2- oil system

Sample	Molecular weight	Temperature (°C)	MMP
Crude oil API 62.1	154	30.34 ± 0.20	890 ± 11.55 psi
n-pentane	72.15	30.36 ± 0.13	680 ± 10.61 psi
n-heptane	100.20	30.36 ± 0.14	785 ± 14.14 psi

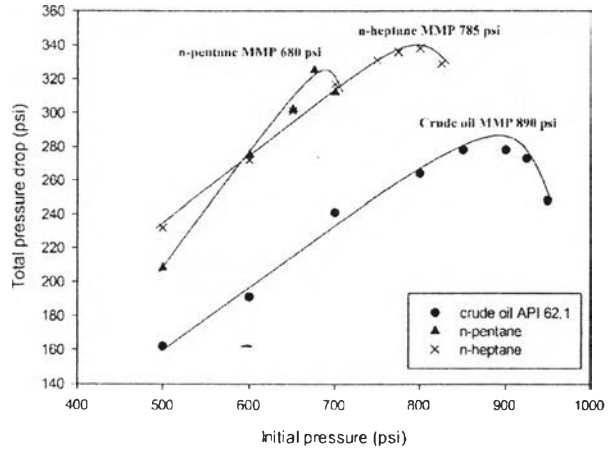

Figure 4.12 Effect of molecular weight on MMP of crude oil API 62.1, n-pentane and n-heptane systems.

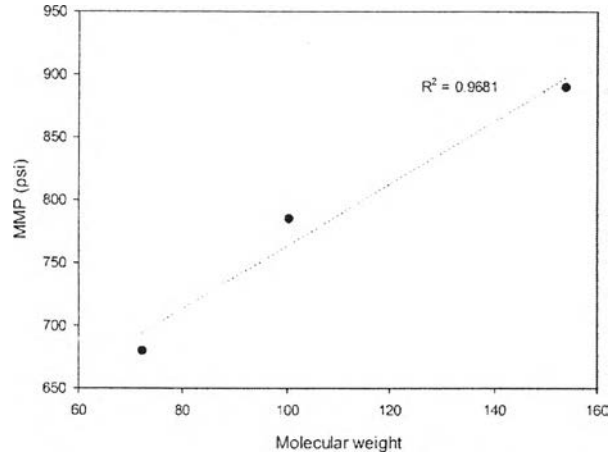

Figure 4.13 Plot of MMP against molecular weight.

At 30 °C, the MMP values of the CO_2-crude oil API 62.1, CO_2-n-pentane, and CO_2-n-heptane systems were 890 psi, 680 psi and 785 psi, respectively. Increase of the oil molecular weight increases the MMP values to all the CO_2-oil system where crude oil API 62.1 was the highest MMP and n-pentane was the lowest. The MMP was related to the viscosity of the oil. Lower viscosity crude oil was benefit to the faster diffusion of CO_2 into the oil. More CO_2 diffuse was easy to extract the light component and reach to the miscible condition. In addition, low molecular weight oil (light oil) was higher the amount of light component than the heavy crude oil.

Lighter component in the oil provides a benefit to get the miscibility condition which was easy to vaporize (extracted) the intermediate components including C_2 to C_6 by the CO_2 at high pressure and form the MCM with vaporizing gas drive. (Li *et al.*, 2012).

With the three data of oil molecular weight and MMP could be generate the correlation between the MMP and oil molecular weight. The effect of molecular weight on MMP was linear function with relative error (R^2) was 0.9681 that was shown in Fig. 4.13. To improve the accuracy of the correlation, it required more data for create a correlation between MMP and molecular weight of crude oil.

4.5 Effect of Temperature on MMP

Effect of temperature on MMP between oil and CO_2 was studied at two different temperature (30 °C and 40 °C). The total pressure drop is plotted against the initial pressure for crude oil API 62.1 and n-heptane and shown in Fig. 4.14 to Fig. 4.15 and the effect of temperature on MMP is shown in Table 4.4.

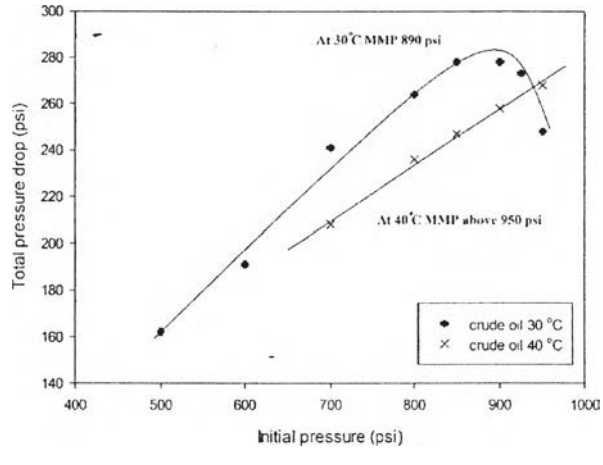

Figure 4.14 Effect of temperature on CO_2- crude oil API 62.1 system.

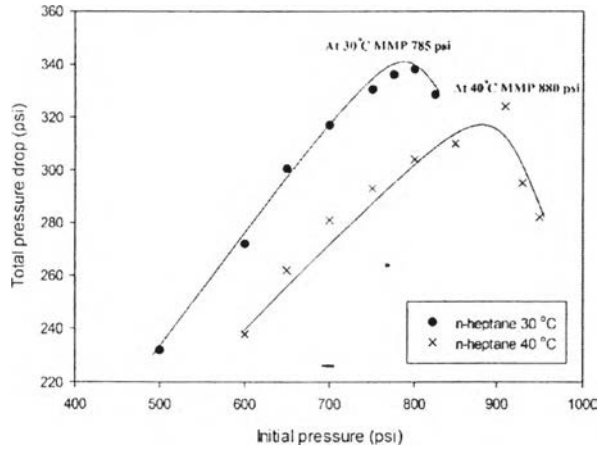

Figure 4.15 Effect of temperature onCO_2- n-heptane system.

Table. 4.4 Effect of temperature on MMP between CO_2 and oil

Sample	Temperature (°C)	MMP from experiment
Crude oil	30.34 ± 0.20	890 psi
	40.36 ± 0.25	Above 950 psi
n-heptane	30.36 ± 0.14	785 psi
	40.23 ± 0.12	880 psi

The MMP of crude oil API 62.1 at 40 °C was is higher than 950 psi which could not be measured in this study because it was beyond the pressure range 400 to 950 psi and the limit of the gas pressure in the CO_2 tank. For the CO_2-n-heptane system, the MMP at 40 °C was 880 psi which was higher than that at 30 °C. Increase temperature increases the MMP of the CO_2-oil system. For crude oil- API 62.1 system, the high temperature induces the vaporization of the oil components that will disturb the multi-contact miscibility between CO_2 and intermediate components which results in increasing the MMP. For the hydrocarbon system (CO_2-C_5 and CO_2-C_7) the solubility of CO_2 is decrease with increasing of temperature due to the expansion of phase envelopment with the result from increase of vapor pressure (Abedini and Torabi, 2013).

4.6 MMP Calculation

To evaluate the results of MMP measured from the pressure decay technique, the MMP values was also calculated using Li *et al.* correlation (2013). It requires MW_{C7+}, X_{VOL}, X_{INT} and T_R which could be obtained from Table 4.5 to calculate MMP and shows the results of the evaluation, the results of MMP from pressure decay technique when comparing with Li *et al.* correlation. The calculated MMP obtained from the correlation of all systems are good agreement with the experimental MMP with percentage absolute error (%AD) less than 10% except that of n-decane system. The calculated MMP of crude oil API 62.1 at 40 °C was 1097 psi, however it could not be obtained in this work due to the limitation of the experimental capacity. Li *et al.* correlation was more accuracy to predict the MMP for light oil and can use to predict the MMP for pure hydrocarbon. But the %AD of n-decane at 20 °C was 20.48%. This prediction was far from the experimental value because in the literature, Li *et al.* correlation was testing with the high temperature (around 100 °C). This correlation wasn't accuracy enough for the prediction at low temperature. This equation should improve the accuracy for calculation in low temperature.

Table 4.5 Comparison of MMPs from this work with Li *et al.* correlation

Sample	T_R (°C)	MW_{C7+}	X_{VOL}	X_{INT}	MMP (psi)		%AD (%)
					This work	Li *et at.*	
Crude oil API 62.1	30.34	145.19	0	0.092	890	878	1.35
	40.36	145.19	0	0.092	Above 950	1097	-
n-pentane	30.36	72.15	0	1	680	640	5.88
n-heptane	30.36	100.20	0	0	785	747	4.84
	40.23	100.20	0	0	880	933	6.02
n-decane	20.40	142.28	0	0	820	652	20.48